Modeling of leakage currents in high-κ dielectrics: Three-dimensional approach via kinetic Monte Carlo

Gunther Jegert,[1,a)] Alfred Kersch,[2] Wenke Weinreich,[3] Uwe Schröder,[4] and Paolo Lugli[1]
[1]*Institute for Nanoelectronics, TU Munich, D-80333 Munich, Germany*
[2]*University of Applied Sciences Munich, D-80335 Munich, Germany*
[3]*Fraunhofer Center Nanoelectronic Technology, D-01099 Dresden, Germany*
[4]*NaMLab gGmbH, D-01099 Dresden, Germany*

(Received 11 December 2009; accepted 18 January 2010; published online 9 February 2010)

We report on a simulation algorithm, based on kinetic Monte Carlo techniques, that allows us to investigate transport through high-permittivity dielectrics. In the example of $TiN/ZrO_2/TiN$ capacitor structures, using best-estimate physical parameters, we have identified the dominant transport mechanisms. Comparison with experimental data reveals the transport to be dominated by Poole–Frenkel emission from donorlike trap states at low fields and trap-assisted tunneling at high fields. © *2010 American Institute of Physics*. [doi:10.1063/1.3310065]

In the most recent generation of metal-oxide-semiconductor devices as well as in storage capacitors of dynamic random access memories high-permittivity (high-κ) dielectrics have replaced SiO_2 as insulator material, since they allow higher capacitance densities and thus enable further downscaling. Unfortunately, high-κ thin films typically suffer from high defect densities, giving rise to trap states that open up pathways for undesirable leakage currents. Especially storage capacitors pose high requirements to the insulating properties of the dielectric. Hence, further scaling requires a detailed understanding of the transport across these films.

Up to now, transport in the most established high-κ materials, ZrO_2 and HfO_2, has been studied using simplified compact-models, e.g., Refs. 1 and 2. In ZrO_2 transport was assumed to be dominated by Poole–Frenkel (PF) emission from traps. According to the standard-PF model (SPF) the current density j is proportional to[3]

$$j \propto F \times \exp\left\{-\frac{1}{k_B T}\left[E_D - \sqrt{e^3 F/(\pi \epsilon_0 \epsilon_{\mathrm{opt}})}\right]\right\}, \tag{1}$$

where E_D is the trap depth measured from the conduction band edge, F is the electric field, and ϵ_{opt} the optical permittivity of the dielectric. However, good fits to experiments could only be achieved by using unrealistic values for material parameters, especially for ϵ_{opt}. This is due to the fact that the picture of charge transport is incomplete. Only charge carrier emission from traps is described, while the injection from the electrodes into the traps is neglected. A tunneling-assisted Poole–Frenkel (TAPF) conduction mechanism has been suggested for HfO_2 (Ref. 4) that incorporates the injection step. However, the TAPF model only considers homogeneous trap distributions and does not take into account that, by applying an electric field, the trap energy becomes a function of the trap position. Furthermore, competing transport channels like detrapping of electrons via quantum mechanical tunneling are not considered.

These restrictions may be lifted by employing Monte Carlo (MC) techniques, which have proven to be a versatile tool for transport simulations.[5–7] Using a kinetic Monte Carlo (kMC) algorithm, we have carried out three-dimensional (3D) tunneling current simulations for metal-insulator-metal (MIM) structures with a high-κ dielectric as insulator. kMC allows us to describe correctly the statistical dynamics of the MIM structure. Individual charge carriers are resolved, whose pathway through the dielectric is tracked. In this way, all relevant transport channels are accounted for concurrently. A 3D description of transport allows us the investigation of arbitrary defect distributions, of spatially localized phenomena (e.g., the formation of percolation paths), and of the influence of rough electrode/dielectric interfaces on the leakage current. Additionally, kMC offers the possibility to study transient phenomena, e.g., charge trapping or degradation, which pose major problems in high-κs.[8]

In the following, only electron transport is discussed, since for the investigated material combination, TiN/ZrO_2, the valence band of the dielectric lies far below the Fermi levels of the electrodes and also far below any defect state relevant for the transport. Thus, hole current as well as population of traps out of the valence band are negligible. Inside the electrodes, acting as electron source/sink, the electron distribution follows Fermi–Dirac statistics. Within the dielectric, electrons are treated as discrete particles with a defined energy, whose trajectory is simulated. At time t the system state is given by the spatial distribution of electrons in the simulated volume of the dielectric. Transport across the dielectric occurs via a series of processes depicted in Fig. 1. As soon as an electron enters the conduction band [either by tunneling (i) or PF emission (vi)], it will be collected at the counter electrode very quickly. The transport time within the

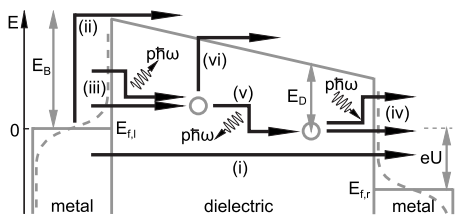

FIG. 1. Schematic band diagram of a MIM structure with applied voltage U. Possible charge transport mechanisms: (i) direct/Fowler–Nordheim tunneling, (ii) thermionic emission, (iii) elastic/inelastic tunneling into and (iv) out of traps, (v) trap-to-trap-tunneling, (vi) PF emission.

a)Electronic mail: guntherjegert@mytum.de.

conduction band is negligible with respect to the time needed by the tunneling processes. For the simulations a kMC algorithm, as proposed by Gillespie,[9] has been adopted, which may be outlined as follows: (I) The simulation is initialized at time $t=0$ by specifying an arbitrary electron distribution. (II) A list of all possible single-electron transitions and their individual rates R is set up and the cumulative transition rate $R_{\mathrm{tot}}=\Sigma_{j=1}^{N}R_j$ is calculated, where N is the number of possible transitions. The transition probabilities are computed by normalizing the corresponding rates against the cumulative transition rate. (III) Employing standard MC sampling techniques,[10] the time increment, i.e., the time the system stays in that state, is determined and the system time is updated. The algorithm randomly selects a transition and executes it with the appropriate probability. (IV) Poisson's equation is solved in the simulation region, since most of the rates depend on the electrostatic potential, which is modified by the charge displacement. By repeating steps (II)–(IV) electron transport through the dielectric is simulated until a steady state is obtained, and leakage current is calculated by counting the electrons that reach the anode in a given time interval. The algorithm itself is only a stochastic procedure and does not contain any information about the involved physics. The quantum mechanical models for the different transport mechanisms, shown in Fig. 1, are wrapped in the transition rates. They will be presented in the following.

Both electrodes emit/absorb electrons. These can either tunnel directly to the counter electrode, or they can be injected into the conduction band of the dielectric by thermionic emission or at high electric fields by Fowler–Nordheim tunneling. The corresponding net rate R_T was derived from the Tsu–Esaki formula for the tunnel current density j_T,[11] using $R_T=j_T*A/e$

$$R_T=\frac{Am_ek_BT}{2\pi^2\hbar^3}\int_0^\infty P(E_t)\ln\left(\frac{1+\exp\left[\frac{-E_t}{k_BT}\right]}{1+\exp\left[\frac{-eU-E_t}{k_BT}\right]}\right)dE_t, \tag{2}$$

whereas A denotes the capacitor area and $P(E_t)$ is the transmission coefficient for electrons with transversal energy E_t, calculated in the Wentzel–Kramers–Brillouin approximation. In the band gap a dispersion relation as proposed by Weinberg has been assumed [see Ref. 12, Eq. (11)], leading to a tunneling mass that is strongly reduced compared to the band masses. The Fermi level of the cathode was set to zero (see Fig. 1). Alternatively, electrons can tunnel into traps, either elastically or inelastically via multiphonon transitions. Elastic tunneling into a defect D occurs with rate[13]

$$R_{CD}^{el}=\frac{8E_1^{1.5}}{3\hbar\sqrt{E_D}}\left(\frac{m_e}{m_{\mathrm{di}}}\right)^{2.5}\times f_C(E)\times P(E), \tag{3}$$

where $f_C(E)$ denotes the Fermi distribution in electrode C, evaluated at trap energy E. Due to the applied bias, E is position-dependent. m_{di} is the effective electron mass in the dielectric material and E_1 is the total energy of the electron in the metal electrode (see Ref. 13). The rate for inelastic multiphonon transitions between electrode C and a defect D at energy E was computed using[14]

$$R_{CD}^{inel}=\int_E^\infty N_C(E')f_C(E')P(E')c_{MP}(E')dE', \tag{4}$$

for trapping of an electron under phonon emission and

$$R_{DC}^{inel}=\int_E^\infty N_C(E')[1-f_C(E')]P(E')e_{MP}(E')dE', \tag{5}$$

for detrapping under phonon absorption, with

$$c_{MP}(E')=\frac{(4\pi)^2r_D^3}{\hbar E_g}\frac{e^2\hbar^2F^2}{2m_{\mathrm{di}}}\sum_{p=0}^{\infty}\delta(E'-E_p)L_p, \tag{6}$$

$$e_{MP}(E')=e^{-(E'-E)/(k_BT)}\times c_{MP}(E'), \tag{7}$$

respectively. Here, N_C is the density of states in electrode C, and $c_{MP}(e_{MP})$ is the capture (emission) rate. $r_D=\hbar/\sqrt{2m_{\mathrm{di}}E_D}$ is the localization radius of the trapped electron,[15] E_g denotes the band gap of the dielectric and L_p is the multiphonon transition probability.[14] $E_p=E+p\hbar\omega$, where ω is the phonon frequency in the one-mode approximation, and p is the number of phonons. Assuming 3D deltalike defect potentials, the rates for elastic defect-defect transitions were calculated from[15,16]

$$R_{DD}^{el}=\nu\times\exp[-2r_{DD}/r_D]. \tag{8}$$

ν is a typical phonon frequency, i.e., about 10^{13} Hz and r_{DD} the distance between the defects. Inelastic multiphonon transitions between two defects were treated according to Ridley.[17] The rate for a transition involving p phonons with energy $\hbar\omega$ is

$$R_{DD}^{MP}=\frac{\pi}{\hbar^2\omega}\times\exp\left[-S(2n+1)-\frac{p\hbar\omega}{2k_BT}\right]\times R_{Rid}. \tag{9}$$

$n=(\exp[(\hbar\omega)/(k_BT)]-1)^{-1}$ is the phonon occupation number and S denotes the Huang–Rhys factor. Evaluation of R_{Rid} is a cumbersome task. Details on this issue and useful approximations can be found in Refs. 17 and 18. Finally, trapped electrons can escape from defect states by PF emission,[3] i.e., field-enhanced thermal emission into the conduction band, with rate[19]

$$R_{\mathrm{PF}}=\nu\times e^{-E_D/k_BT}\left\{\frac{1}{\beta^2}[1+(\beta-1)e^{\beta}]+\frac{1}{2}\right\}, \tag{10}$$

whereas $\beta=\sqrt{Ze^3F/(\pi\epsilon_0\epsilon_{opt}k_B^2T^2)}$ and Z is the charge of the left-behind defect.

Figure 2 shows a comparison of the simulation results with experimental leakage data of a TiN/ZrO_2/TiN capacitor structure. 9 nm of ZrO_2 were grown by atomic layer deposition (TEMAZ, O_3) at 275 °C on silicon wafers coated with chemical vapor-deposited (CVD) TiN ($TiCl_4$,NH_3), grown at 550 °C. The top TiN electrode was deposited at 450 °C by CVD. Current measurements were carried out with a Keithley 4200 parameter analyzer.[20] For electric fields lower than about 1.5 MV/cm measured currents were of the order of picoamperes, i.e., below the measuring sensitivity. The dotted lines show the best fit via the SPF model, see Eq. (1). A good fit at low fields could only be achieved assuming an optical permittivity of $\epsilon_{opt}=2$, which is far below the expected value of 5.6.[21] Otherwise, the calculated slopes of the leakage current would be too low. The failure of the SPF model is due to the fact that it neglects carrier injection into

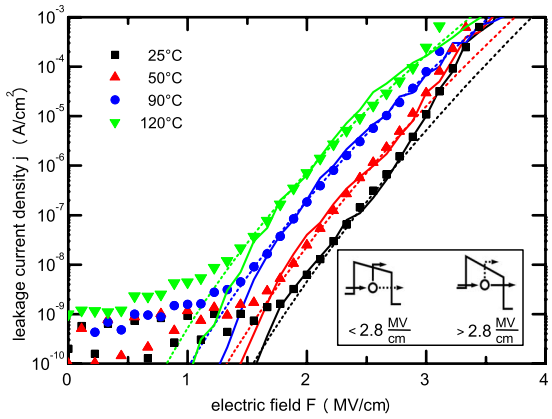

FIG. 2. (Color online) Leakage current data (from Ref. 20) of a $TiN/ZrO_2/TiN$ capacitor with a 9 nm dielectric. Dielectric breakdown was observed for $E \geq 3.5$ MV/cm (not shown). Continuous lines show kMC simulation results, dotted lines evaluation with the standard PF compact-model.

the traps. Within this model, transport is purely bulk-limited, and the influence of the electrode is neglected. Our simulation shows that, depending on the applied voltage, traps at different distances from the injecting electrode deliver the dominant contribution to the leakage current, as the alignment of the trap states with respect to the Fermi level of the electrode changes. At high fields, especially at the lowest temperatures shown in Fig. 2, the SPF model underestimates the current. These deficiencies are removed in kMC simulations. Although the presented algorithm can handle multiple trap levels with arbitrary spatial distribution, the best fit, shown in Fig. 2, was achieved using a relatively simple model with a single trap level and a homogeneous trap density of 3×10^{18} cm^{-3}. Further fixed parameters were $\epsilon_{opt}=5.6$, $E_g=5.4$ eV, $S=1$, $\omega=40$ meV,[21] $m_{cb}=1.2m_e$, and $m_{vb}=2.5m_e$.[22] Only the conduction band offset E_B between TiN and ZrO_2 and the trap depth E_D were varied. Best fit was achieved for defects at $E_D=1.15$ eV, which, in unoccupied state, are positively charged, and $E_B=1.74$ eV. According to the metal induced gap states (MIGS) model,[23] assuming a work function of 4.7 eV for TiN,[24] an electron affinity of 2.5 eV and a charge neutrality level of 3.6 eV for ZrO_2,[23] a barrier of 1.45 eV is calculated. Since the MIGS model tends to overestimate the barrier reduction due to Fermi level pinning for wide gap oxides,[25] the extracted value seems reasonable. According to the kMC simulations, at higher fields ($\geq$2.8 MV/cm) a transition from PF conduction to trap-assisted tunneling (TAT) takes place (see inset Fig. 2), leading to a reduced temperature dependence of the current. For increasing temperature this transition shifts to higher fields, since PF conduction has a more pronounced temperature dependence then the nearly temperature-independent TAT. TAT is not considered in the SPF model, which thus underestimates the current.

In summary, a kinetic Monte Carlo approach toward the 3D modeling of leakage currents in high-κ dielectrics has been presented. Simulation results have been compared to experimental data of $TiN/ZrO_2/TiN$ capacitor structures and a model for the transport has been deduced that, in contrast to standard models, does not invoke unphysical parameters like extremely low optical permittivities. Leakage current has been found to mainly flow across donorlike trap states.

[1] Y. Seo, S. Lee, I. An, C. Song, and H. Jeong, Semicond. Sci. Technol. **24**, 115016 (2009).
[2] S. Chakraborty, M. K. Bea, G. K. Dalapti, D. Paramanik, S. Varma, P. K. Bose, S. Bhattacharya, and C. K. Maiti, Semicond. Sci. Technol. **21**, 467 (2006).
[3] J. R. Yeargan and H. L. Taylor, J. Appl. Phys. **39**, 5600 (1968).
[4] D. S. Jeong and C. S. Hwang, J. Appl. Phys. **98**, 113701 (2005).
[5] C. Jacoboni and P. Lugli, *The Monte Carlo Method for Semiconductor Device Simulation* (Springer, New York, 1989).
[6] M. Zebarjadi, C. Bulutay, K. Esfarjani, and A. Shakouri, Appl. Phys. Lett. **90**, 092111 (2007).
[7] C. Jirauschek and P. Lugli, J. Appl. Phys. **105**, 123102 (2009).
[8] D. Zhou, U. Schröder, G. Jegert, M. Kerber, S. Uppal, R. Agaiby, M. Reinicke, J. Heitmann, and L. Oberbeck, J. Appl. Phys. **106**, 044104 (2009).
[9] D. T. Gillespie, J. Comput. Phys. **22**, 403 (1976).
[10] K. A. Fichthorn and W. H. Weinberg, J. Chem. Phys. **95**, 1090 (1991).
[11] R. Tsu and L. Esaki, Appl. Phys. Lett. **22**, 562 (1973).
[12] Z. A. Weinberg, J. Appl. Phys. **53**, 5052 (1982).
[13] X. R. Cheng, Y. C. Cheng, and B. Y. Liu, J. Appl. Phys. **63**, 797 (1988).
[14] M. Herrmann and A. Schenk, J. Appl. Phys. **77**, 4522 (1995).
[15] G. Lucovsky, Solid State Commun. **3**, 299 (1965).
[16] H. Krause, Phys. Status Solidi A **62**, 565 (1979).
[17] B. K. Ridley, J. Phys. C **11**, 2323 (1978).
[18] B. K. Ridley, Solid-State Electron. **21**, 1319 (1978).
[19] J. L. Hartke, J. Appl. Phys. **39**, 4871 (1968).
[20] For details of the growth process see: W. Weinreich, R. Reiche, M. Lemberger, G. Jegert, J. Müller, L. Wilde, S. Teichert, J. Heitmann, E. Erben, L. Oberbeck, U. Schröder, A. J. Bauer, and H. Ryssel, Microelectron. Eng. **86**, 1826 (2009).
[21] G.-M. Rignanese, F. Detraux, X. Gonze, and A. Pasquarello, Phys. Rev. B **64**, 134301 (2001).
[22] J. E. Medvedeva, A. J. Freeman, C. B. Geller, and D. M. Rishel, Phys. Rev. B **76**, 235115 (2007).
[23] J. Robertson, J. Vac. Sci. Technol. B **18**, 1785 (2000).
[24] K. Xiong, J. Robertson, G. Pourtois, J. Pétry, and M. Müller, J. Appl. Phys. **104**, 074501 (2008).
[25] J. Robertson, J. Vac. Sci. Technol. B **27**, 277 (2009).